

Effect of storm-time plasma pressure on the magnetic field in the inner magnetosphere

Sorin Zaharia, M. F. Thomsen, J. Birn, and M. H. Denton

Los Alamos National Laboratory, Los Alamos, New Mexico, USA

V. K. Jordanova

Space Science Center, University of New Hampshire, Durham, New Hampshire, USA

C. Z. Cheng

Princeton Plasma Physics Laboratory, Princeton University, Princeton, New Jersey, USA

Received 14 September 2004; revised 8 December 2004; accepted 5 January 2005; published 2 February 2005.

[1] We investigate the effect of plasma pressure on the magnetic field in the near-Earth magnetosphere (2 to 6.5 R_E) during the major magnetic storm of October 21–25, 2001. For this we obtain a time series of “snapshots”, in each of which the magnetic forces are equilibrated by plasma pressure gradient forces. Each snapshot is computed using our 3-D equilibrium code, which is fed anisotropic pressure in the equatorial plane from a kinetic ring current model. As computational boundaries we use magnetic flux surfaces obtained from the T89 empirical model [Tsyganenko, 1989], parameterized by the appropriate K_p . We analyze the computed magnetic fields and electric currents at each stage of the storm. Our findings include significant (~ 10) plasma β and large field depressions near Earth at the storm peak. The results clearly show the necessity of a magnetically self-consistent treatment of plasma transport in storm modeling. **Citation:** Zaharia, S., M. F. Thomsen, J. Birn, M. H. Denton, V. K. Jordanova, and C. Z. Cheng (2005), Effect of storm-time plasma pressure on the magnetic field in the inner magnetosphere, *Geophys. Res. Lett.*, 32, L03102, doi:10.1029/2004GL021491.

1. Introduction

[2] During intense magnetic storms, observations [e.g., Tsyganenko *et al.*, 2003] show deep magnetic field depressions even very close to Earth ($L \sim 3-4$). Since the dipole field is used extensively in storm modeling, it is important to quantify the degree to which it is inadequate (i.e., the importance of the ring current in changing the field) during such events. One way to do this is by empirical modeling — which is not always the right solution, especially for applications in which equilibrium between field and plasma is required [Zaharia and Cheng, 2003b]. Another way is computing magnetospheric structures in which the field is force balanced with the plasma pressure.

[3] Two numerical 3-D equilibrium approaches exist that include the near-Earth region: a “magnetofriction” MHD approach [Hesse and Birn, 1993; Toffoletto *et al.*, 2001] and an iterative solution in flux coordinates (Euler potentials) that uses prescribed pressure at one point on the field lines [Cheng, 1995; Zaharia and Cheng, 2003a; Zaharia *et al.*, 2004]. While both techniques have been successfully

applied to isotropic pressure cases, the former has not been extended to anisotropic pressure. Since near-Earth plasma pressure is anisotropic ($P_{\perp} > P_{\parallel}$) during both quiet and active times [e.g., De Michelis *et al.*, 1999], the latter approach is currently the only available tool of finding 3-D equilibria with anisotropic pressure.

[4] Previous studies with this approach [Zaharia *et al.*, 2004] have used statistical pressure/degree of anisotropy observations [Lui *et al.*, 1994; De Michelis *et al.*, 1999].

[5] Here we compute a sequence of near-Earth equilibria on shorter time scales, during a magnetic storm, with input pressure from a kinetic model at one-hour intervals. While the pressure employed is perhaps not entirely realistic, being obtained by using a dipolar field (and thus we cannot claim that the obtained configurations will accurately reproduce observations), the study will give an indication of how strongly the field gets deformed by the plasma pressure, and thus of how good the dipolar approximation is in the near-Earth magnetosphere during storms.

[6] The study considers the intense ($Dst < -150$ nT) storm of October 21–25, 2001, which was simulated using the UNH-RAM model, a kinetic ring current model analyzing the bounce-averaged motion in a dipolar \mathbf{B} -field, including

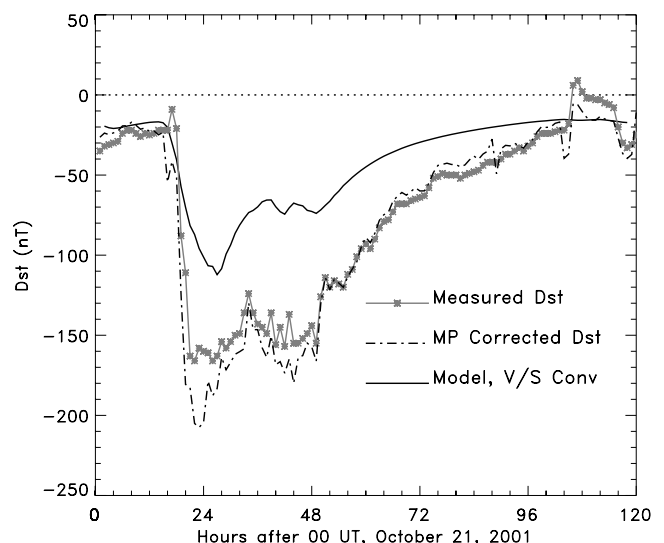


Figure 1. Measured and modeled DST index during the intense magnetic storm of October 21–25, 2001.

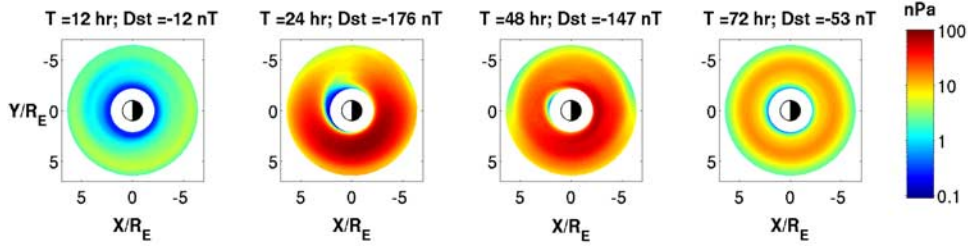


Figure 2. Equatorial profiles of P_{\perp} (nPa) inside circular sectors of radii $2 R_E$ and $6.5 R_E$ at four hours during the storm.

convection and various loss processes [Jordanova *et al.*, 1997]. The model takes initial conditions from POLAR/MICS data and boundary conditions from LANL/MPA and SOPA data. In Figure 1 we show the measured/modeled Dst for this storm (the RAM model uses K_p -dependent Volland-Stern convection for all results here, with the coefficient $A(K_p)$ presented by Jordanova *et al.* [1998, Figure 4]).

[7] Our results show the force-balanced \mathbf{B} -field to be significantly depressed compared to the dipole field during this storm. We find that plasma β (the ratio of plasma to magnetic pressure) can be very large (~ 10) even as close as $5 R_E$ from Earth, requiring strong field-line stretching to accommodate force balance. The results demonstrate the need for improving the magnetic fields used in storm-time kinetic modeling, ideally by feeding the kinetic models fields computed to be in force balance with the plasma distribution. While not yet fully self-consistent in that the equilibrium field is not returned to the kinetic simulation to guide its continued evolution, the work here also represents a first step toward adding that self-consistency to a global kinetic ring current model.

2. Model

[8] The equilibrium with anisotropic pressure is an extension [Zaharia, 2003] of the isotropic case [Cheng, 1995; Zaharia *et al.*, 2004]. The 3-D force balance equation is decomposed (by expressing \mathbf{B} in terms of Euler potentials as $\mathbf{B} = \nabla\psi \times \nabla\alpha$) into two “quasi-2D” elliptic PDEs for ψ and α , which are (in the rationalized EMU system):

$$\nabla \cdot \left[(\nabla\psi)^2 \nabla\alpha - (\nabla\alpha \cdot \nabla\psi) \nabla\psi \right] = - \frac{(\mathbf{B} \times \nabla\psi)}{\sigma B^2} \cdot \left[\nabla P_{\perp} + (1 - \sigma) \nabla \left(\frac{B^2}{2} \right) \right] \quad (1)$$

$$\nabla \cdot \left[(\nabla\alpha \cdot \nabla\psi) \nabla\alpha - (\nabla\alpha)^2 \nabla\psi \right] = - \frac{(\mathbf{B} \times \nabla\alpha)}{\sigma B^2} \cdot \left[\nabla P_{\perp} + (1 - \sigma) \nabla \left(\frac{B^2}{2} \right) \right], \quad (2)$$

where $\sigma = 1 + (P_{\perp} - P_{\parallel})/B^2$ (note: the Euler potentials ψ and α are usually referred to as α and β , respectively, in the space physics community). The equations are solved iteratively, with the non-linear right hand side terms kept fixed at each iteration. For a unique solution, one needs the pressures P_{\perp} and P_{\parallel} at one point on each field line, as well as boundary conditions (BCs) for the magnetic flux ψ , together with the shapes of the inner/outer flux surfaces (the BC for α is periodicity). The BCs in the third coordinate χ (along the field lines) is simply that the ψ and α potentials at each end of the line (i.e. on the Earth surface) are those of a dipole, which are analytically known.

[9] The boundary shapes for ψ are usually obtained by field-line tracing using empirical models [Zaharia *et al.*, 2004]. Here we use the T89 model (chosen mainly because the RAM model uses K_p -dependent convection), parameterized by the nearest integer corresponding to the observed K_p at each hour of the storm. We thus build 6 computational domains (with K_p from 1 to 6), covering different times throughout the storm. Although the T89 field is also taken as an initial “guess,” the computed field will be different from it everywhere: while inside the domain the field lines “move” with three degrees of freedom as they approach equilibrium, on the boundaries they still retain two degrees of freedom — they can slide on the boundaries to accommodate the pressure gradients).

[10] The pressure input consists of equatorial P_{\perp} and P_{\parallel} which are moments of the distribution function from the kinetic model. Only the ion (H^+ , O^+ and He^+) pressure is

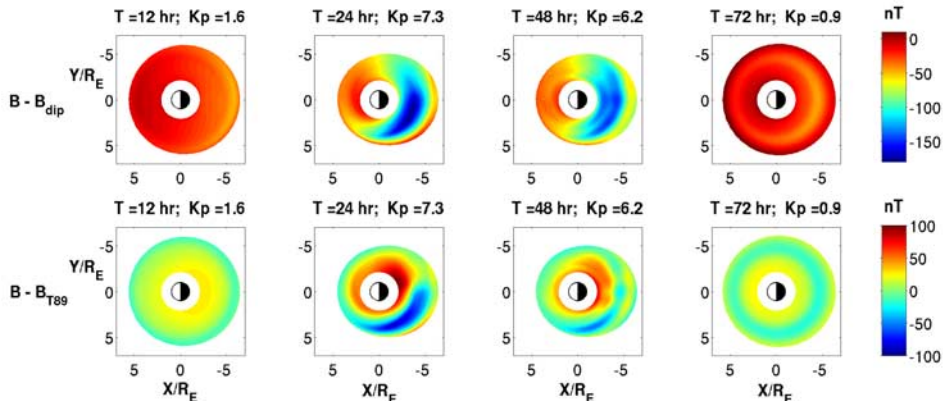


Figure 3. Equatorial profiles of $B - B_{dip}$ (top) and $B - B_{T89}$ (bottom) (B is the computed field) at four different times.

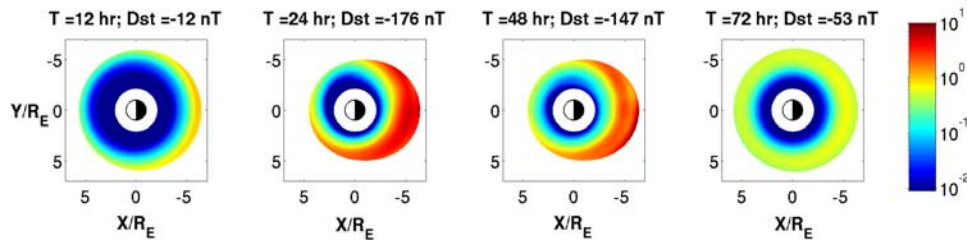


Figure 4. Plasma β_{\perp} on the equatorial plane at the four chosen times throughout the storm.

considered, with the electron pressure neglected. While for the isotropic case the pressure can simply be “mapped” along the field lines as in equilibrium it is constant along them, this is not so for anisotropy. However, for bi-Maxwellian pressure in a collisionless plasma we can use energy and magnetic moment conservation to find the pressure along the field lines at each iteration [e.g., *Spence et al.*, 1987; *Zaharia*, 2003]. We note that the pressure profile is kept spatially fixed in the equatorial plane, and therefore $P_{\perp}(\psi, \alpha, \chi)$ and $P_{\parallel}(\psi, \alpha, \chi)$ change at each iteration until equilibrium is achieved. Thus the obtained 3-D equilibria also provide a mapping of the equatorial P_{\perp} and P_{\parallel} into the whole domain.

[11] Pressure data were available from the RAM model for 120 hours, starting at 00:00 UT on October 21, 2001, and one equilibrium “snapshot” was computed for each hour (we only present results at four of those hours here). The equatorial P_{\perp} , shown at these times in Figure 2, greatly increases at the peak of the storm, reaching more than 90 nPa in the dusk sector at $4 R_E$. Before the storm, as well as in the recovery phase, the pressure is nowhere larger than 12 nPa. The degree of anisotropy P_{\perp}/P_{\parallel} (not shown) is large close to Earth at the peak of the storm and in the recovery phase (when it exceeds 5).

3. Results

[12] Unlike our previous study which extended to $23 R_E$ from Earth [*Zaharia et al.*, 2004], the computations here are from $2 R_E$ to $6.5 R_E$ only. Each equilibrium snapshot is computed in one of six domains, built using T89 with K_p the nearest integer corresponding to the measured K_p . While all six domains extend to $6.5 R_E$ at midnight, they are more or

less compressed at other longitudes, due to the different magnetic flux compression at different K_p .

[13] Figure 3 shows equatorial plane profiles of the difference between the computed and the dipolar and T89 magnetic fields, respectively: $B - B_{dip}$ and $B - B_{T89}$. It is clear that the computed field is much lower than dipolar. The minimum $B - B_{dip}$ (-170 nT) is attained at $T = 24$ hr, at $4 R_E$ from Earth in the nightside. The T89 field is itself different from dipolar, but the bottom plots show that the computed field is also different from the T89 field, with the largest difference again at the peak of the storm, when the field inside the domain exhibits the largest depression (-100 nT) compared to the T89 field.

[14] Figure 4 shows plasma β_{\perp} in the equatorial plane. While β_{\perp} is low (generally <1) before the storm/in the recovery phase, it greatly increases at its peak, reaching a value of about 10 on the night side. This explains why the field is so changed from a dipole, as when $\beta > 1$ the pressure is crucial in determining the magnetic configuration.

[15] Figure 5 shows the azimuthal current density J_{ϕ} in the equatorial and noon-midnight meridian planes. One clearly sees two current systems, one eastward at $\sim 3 R_E$, the other westward at $4-6 R_E$, in agreement with observations [e.g., *Le et al.*, 2004]. The largest currents (~ 20 nA/m²) are at dusk, in locations of high pressure. They are largest at the storm peak, with $J_{\phi, \max}$ more than an order of magnitude larger than before the storm. An interesting feature in the noon-midnight meridian plots is that at the storm peak, instead of having maximum in the equatorial plane, the westward current on the nightside has a “butterfly” shape, with maxima above and below the plane. This is due to the pressure anisotropy: a current in an equilibrium with anisotropic pressure is lower where β_{\perp} is higher [*Hoffman*

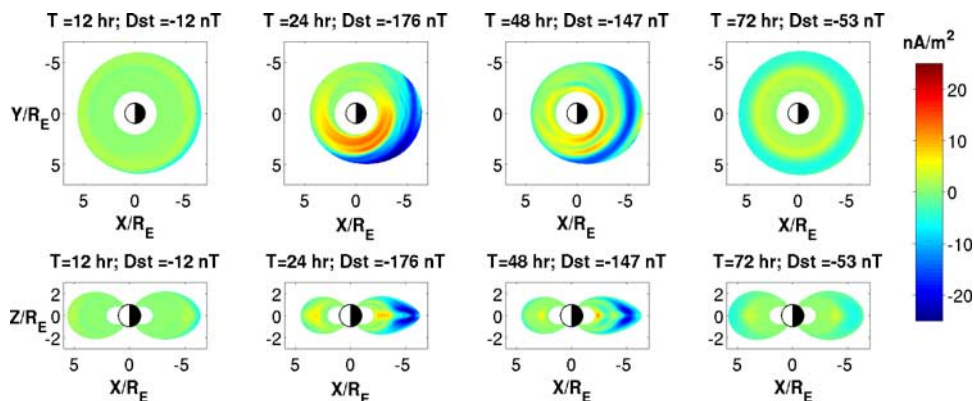


Figure 5. Azimuthal current density J_{ϕ} (nA/m²) in the (top) equatorial and (bottom) noon-midnight meridian planes. Positive (negative) signs show currents that are eastward (westward) in the night side.

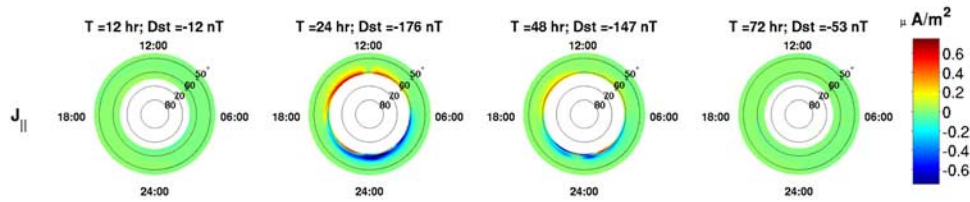


Figure 6. Field-aligned current density J_{\parallel} ($\mu\text{A}/\text{m}^2$) at the top of the ionosphere. Positive (negative) signs show currents into (out of) the ionosphere. The computational domain extends to higher ionospheric latitudes for lower Kps .

and Bracken, 1967; Cowley, 1978; Cheng, 1992]. Indeed, writing

$$J_{\phi} \approx -\frac{R}{\sigma B^2} (\mathbf{B} \times \nabla \alpha) \cdot \left[\nabla P_{\perp} + (1 - \sigma) \nabla \left(\frac{B^2}{2} \right) \right] \quad (3)$$

one notices a term, proportional to $(1 - \sigma)$, opposite to the main current. Farther in the tail this term can become so large in the equatorial plane that a strong bifurcation of the current takes place [Zaharia et al., 2004].

[16] Finally, Figure 6 shows the Birkeland current density J_{\parallel} at the top of the ionosphere. J_{\parallel} is negligible before the storm and in the recovery phase, but increases to $\sim 1 \mu\text{A}/\text{m}^2$ at its peak (this is significant, as all latitudes here map to less than $6.5 R_E$ from Earth). There is also a clear equatorward drift of the currents at the storm peak.

4. Summary and Discussion

[17] In order to quantify the effect of plasma pressure on the magnetic field during a storm, in this paper we present a time series of 3-D equilibrium “snapshots” of the inner magnetosphere during the magnetic storm of October 21, 2001. The snapshots are computed using magnetic flux boundaries obtained from the T89 empirical magnetospheric field model and prescribed anisotropic pressure from the UNH-RAM ring current kinetic model.

[18] A major result of the study is that during intense storms plasma β_{\perp} can be significant (~ 10). This shows that plasma pressure strongly affects the \mathbf{B} -field even very close to Earth during such events. Other results include very large azimuthal current density ($\sim 20 \text{ nA}/\text{m}^2$), with concomitant increase in the field-aligned currents at the ionosphere. Due to the high β_{\perp} there are large \mathbf{B} -field depressions compared to a dipolar field (and a decrease even from the T89 field). Other computations (not presented here), with dipole flux boundary conditions, also show high β_{\perp} (~ 2) and large magnetic field depressions, thus clearly showing that the dipolar approximation breaks down during intense storms and indicating the necessity of a magnetically self-consistent treatment of plasma transport.

[19] We note that the RAM model with Volland-Stern electric convection underestimates the Dst index (see Figure 1) and thus likely the pressures as well. We found that using the more realistic Weimer 01 convection model leads to a better reproduction of the Dst . Therefore, more detailed work, to be addressed in a forthcoming JGR paper, will include pressure input from the kinetic model with Weimer 01 convection, as well as the use of the more realistic Tsyganenko T01 “storm” model [Tsyganenko et al., 2003] for obtaining the flux BCs. The present modeling

is a first step toward adding self-consistency to the RAM model by feeding it magnetic field computed to be in force balance with the model-derived plasma pressure.

[20] **Acknowledgments.** This work was performed under the auspices of the U.S. Department of Energy, with LANL support for S. Zaharia in the form of an LDRD Director’s Fellowship. Additional support is acknowledged from the DOE Office of Basic Energy Sciences, the NASA’s Sun Earth Connection Theory Program and the National Science Foundation through grants ATM-0202306 and ATM-0309585.

References

- Cheng, C. Z. (1992), Magnetospheric equilibrium with anisotropic pressure, *J. Geophys. Res.*, *97*, 1497.
- Cheng, C. Z. (1995), Three-dimensional magnetospheric equilibrium with isotropic pressure, *Geophys. Res. Lett.*, *22*, 2401.
- Cowley, S. W. H. (1978), The effect of pressure anisotropy on the equilibrium structure of magnetic current sheets, *Planet. Space Sci.*, *26*, 1037.
- De Michelis, P., et al. (1999), An average image of proton plasma pressure and of current systems in the equatorial plane derived from AMPTE/CCE-CHEM measurements, *J. Geophys. Res.*, *104*, 28,615.
- Hesse, M., and J. Birn (1993), Three-dimensional magnetotail equilibria by numerical relaxation techniques, *J. Geophys. Res.*, *98*, 3973.
- Hoffman, R. A., and P. A. Bracken (1967), Higher-order ring currents and particle energy storage in the magnetosphere, *J. Geophys. Res.*, *72*, 6039.
- Jordanova, V. K., et al. (1997), Kinetic model of the ring current-atmosphere interactions, *J. Geophys. Res.*, *102*, 14,279.
- Jordanova, V. K., et al. (1998), October 1995 magnetic cloud and accompanying storm activity: Ring current evolution, *J. Geophys. Res.*, *103*, 79.
- Le, G., et al. (2004), Morphology of the ring current derived from magnetic field observations, *Ann. Geophys.*, *22*, 1267.
- Lui, A. T. Y., et al. (1994), Empirical modeling of the quiet time nightside magnetosphere, *J. Geophys. Res.*, *99*, 151.
- Spence, H. E., et al. (1987), Static magnetic field models consistent with nearly isotropic plasma pressure, *Geophys. Res. Lett.*, *14*, 872.
- Toffoletto, A. F., et al. (2001), Modeling inner magnetospheric electro-dynamics, in *Proceedings of the Chapman Conference on Space Weather*, edited by P. Song, G. L. Siscoe, and H. J. Singer, p. 313, AGU, Washington, D. C.
- Tsyganenko, N. A. (1989), A magnetospheric field model with a warped tail current sheet, *Planet. Space Sci.*, *37*, 5.
- Tsyganenko, N. A., et al. (2003), Storm-time distortion of the inner magnetosphere: How severe can it get?, *J. Geophys. Res.*, *108*(A5), 1209, doi:10.1029/2002JA009808.
- Zaharia, S. (2003), 3-D magnetospheric structures and energetic particle injections, Ph.D. thesis, Princeton Univ., Princeton, N. J.
- Zaharia, S., and C. Z. Cheng (2003a), Near-Earth thin current sheets and Birkeland currents during substorm growth phase, *Geophys. Res. Lett.*, *30*(17), 1883, doi:10.1029/2003GL017456.
- Zaharia, S., and C. Z. Cheng (2003b), Can an isotropic plasma pressure distribution be in force balance with the T96 model field?, *J. Geophys. Res.*, *108*(A11), 1412, doi:10.1029/2002JA009501.
- Zaharia, S., et al. (2004), 3-D force-balanced magnetospheric configurations, *Ann. Geophys.*, *22*, 251, SRef-ID:#1432-0576/ag/2004-22-251.

J. Birn, M. H. Denton, M. F. Thomsen, and S. Zaharia, Los Alamos National Laboratory, P.O. Box 1663, MS D466, Los Alamos, NM 87545, USA. (szaharia@lanl.gov)

C. Z. Cheng, Princeton Plasma Physics Laboratory, Princeton University, Princeton, NJ 08543, USA.

V. K. Jordanova, Space Science Center, University of New Hampshire, Durham, NH 03824, USA.